Journal of Neurochemistry

JOURNAL OF NEUROCHEMISTRY | 2011

doi: 10.1111/j.1471-4159.2011.07178.x

Adenosine A_{2A} receptors control neuroinflammation and consequent hippocampal neuronal dysfunction

Nelson Rebola,*[1] Ana Patrícia Simões,*[1] Paula M. Canas,*[1] Angelo R. Tomé,*,† Geanne M. Andrade,* Claire E. Barry,‡ Paula M. Agostinho,* Marina A. Lynch‡ and Rodrigo A. Cunha*

*Center for Neuroscience of Coimbra, Institute of Biochemistry, Faculty of Medicine, University of Coimbra, Coimbra, Portugal

†Department of Life Sciences, Faculty of Science and Technology, University of Coimbra, Coimbra, Portugal

‡Department of Physiology, Trinity College, Dublin, Ireland

Abstract

The blockade of adenosine A_{2A} receptors (A2AR) affords a robust neuroprotection in different noxious brain conditions. However, the mechanisms underlying this general neuroprotection are unknown. One possible mechanism could be the control of neuroinflammation that is associated with brain damage, especially because A2AR efficiently control peripheral inflammation. Thus, we tested if the intracerebroventricular injection of a selective A2AR antagonist (SCH58261) would attenuate the changes in the hippocampus triggered by intraperitoneal administration of lipopolysaccharide (LPS) that induces neuroinflammation through microglia activation. LPS administration triggers an increase in inflammatory mediators like interleukin-1β that causes biochemical changes (p38 and c-jun N-terminal kinase phosphorylation and caspase 3 activation) contributing to neuronal dysfunction typified by decreased long-term potentiation, a form of synaptic plasticity. Long-term potentiation, measured 30 min after the tetanus, was significantly lower in LPS-treated rats compared with control-treated rats, while SCH58261 attenuated the LPS-induced change. The LPS-induced increases in phosphorylation of c-jun N-terminal kinase and p38 and activation of caspase 3 were also prevented by SCH58261. Significantly, SCH58261 also prevented the LPS-induced recruitment of activated microglial cells and the increase in interleukin-1β concentration in the hippocampus, indicating that A2AR activation is a pivotal step in mediating the neuroinflammation triggered by LPS. These results indicate that A2AR antagonists prevent neuroinflammation and support the hypothesis that this mechanism might contribute for the ability of A2AR antagonists to control different neurodegenerative diseases known to involve neuroinflammation.

Keywords: A_{2A} receptors, adenosine, long-term potentiation, microglia, neuroinflammation.

J. Neurochem. (2011) 10.1111/j.1471-4159.2011.07178.x

Neurological diseases account for approximately 30% of the total disease burden in Europe and neurodegenerative diseases account for a significant proportion of these (Olesen and Leonardi 2003). The neuromodulation system operated by adenosine has received an increasing attention as a potential novel target to manage neurodegenerative conditions, in view of its combined neuronal, glial and vascular effects (reviewed in Fredholm *et al.* 2005). This is best exemplified by the current development (phase IIb) of adenosine A_{2A} receptor (A2AR) antagonists as anti-Parkin-

Received February 28, 2010; revised manuscript received November 30, 2010; accepted January 5, 2011.

Address correspondence and reprint requests to Rodrigo A. Cunha, Center for Neuroscience of Coimbra, Institute of Biochemistry, Faculty of Medicine, University of Coimbra, 3004-504 Coimbra, Portugal.
E-mail: cunharod@gmail.com

[1]These authors contributed equally to the experimental effort of this study.

Abbreviations used: A1R, A1 receptor; A2AR, A2A receptor; BSA, bovine serum albumin; DPCPX, 1,3-dipropyl-8-cyclopentylxanthine; EPSP, excitatory post-synaptic potentials; IR, immunoreactivity; iNOS, inducible nitric oxide synthase; JNK, c-jun N-terminal kinase; LPS, lipopolysaccharide; LTP, long-term potentiation; MSX-3, 3,7-dihydro-8-[(1E)-2-(3-methoxyphenyl)ethenyl]-7-methyl-3-[3-(phosphonooxy)propyl-1-(2-propynyl)-1H-purine-2,6-dione disodium salt hydrate; PBS, phosphate-buffered saline; SCH58261, 5-amino-7-2-phenylethyl.-2-2-furyl-pyrazolo[4,3-ex-1,2,4-triazolo-1,5-9-pyrimidine; SDS, sodium dodecyl sulfate; TBS, Tris-buffered saline; vGAT, vesicular GABA transporter; vGluT1 and vGluT2, glutamate transporters types 1 and 2; XAC, 8-{4-[(2-aminoethyl)amino]carbonylmethyl-oxyphenyl}xanthine.

sonian drugs, based on their simultaneous ability to normalize motor function and to afford a marked neuroprotection (Xu *et al.* 2005). This neuroprotection afforded by A2AR blockade is also observed in animal models of different other neurodegenerative disorders such as Huntington's disease, Alzheimer's disease, epilepsy and excitotoxic conditions including ischemia (reviewed in Cunha 2005; Chen *et al.* 2007). However, the mechanisms by which A2AR control brain damage are currently unknown, but they are expected to be either different concurring mechanisms or instead general mechanisms given the broad spectrum of neurodegenerative conditions where A2AR blockade is neuroprotective (discussed in Cunha 2005; Chen *et al.* 2007).

One possibility would be that A2AR might control neuroinflammation, a common event in neurodegenerative diseases, characterized by the appearance of activated inflammatory microglial cells and increase in the levels of inflammatory mediators (Allan *et al.* 2005; Marchetti and Abbracchio 2005). In fact, microglial activation is a faithful sensor of pathologic events in the brain (Kreutzberg 1996) and a decrease in the extent of neuroinflammation is associated with a better prognosis in the progression of neurodegenerative diseases (Allan *et al.* 2005; Marchetti and Abbracchio 2005). The role of A2AR in the control of neuroinflammation is currently unclear although this suggestion is consistent with the observation that A2AR are the main OFF signal of peripheral inflammation (reviewed in Sitkovsky and Ohta 2005). Studies in animal models of Parkinson's disease (Pierri *et al.* 2005; Yu *et al.* 2008) and traumatic brain injury (Dai *et al.* 2010) suggest that A2AR blockade control microglial activation; however, other studies using primary cultures of microglia cells have reached opposite conclusions related to control of function by A2AR (Saura *et al.* 2005; Orr *et al.* 2009; van der Putten *et al.* 2009; Dai *et al.* 2010), questioning a direct role of A2AR in the control of neuroinflammation in an *in vivo* setting.

This study was designed to test if the blockade of A2AR could prevent the biochemical, morphological and functional consequences of an experimentally induced neuroinflammation triggered by administration of lipopolysaccharide (LPS). This toxin from Gram negative bacteria is a prototypical trigger of inflammation and is known to be a potent trigger of neuroinflammation (e.g. Kim *et al.* 2000; Chakravarty and Herkenham 2005); furthermore, we have already carried out considerable work to understand the relation between the genesis of neuroinflammation, caused by LPS, and neuronal dysfunction using long-term potentiation (LTP) in the hippocampus as readout (Vereker *et al.* 2000; Kelly *et al.* 2003; Nolan *et al.* 2003).

Methods

Drugs

LPS from *Escherichia coli* (serotype 055:B5) was from Sigma (St Louis, MO, USA), the kit for ELISA quantification of interleukin 1β (Duoset) was acquired from Genzyme Diagnostics, 5-amino-7-(2-phenylethyl)-2-(2-furyl)-pyrazolo[4,3-e]-1,2,4-triazolo[1,5-c]pyrimidine (SCH58261) was a generous gift from Scott Weiss (Vernalis, UK) and 3,7-dihydro-8-[(1E)-2-(3-methoxyphenyl)ethenyl]-7-methyl-3-[3-(phosphonooxy)propyl-1-(2-propynyl)-1H-purine-2,6-dione disodium salt hydrate (MSX-3) was a generous gift from Sergi Ferre (NIDA, USA).

Animals and experimental groups

Groups of male Wistar rats (300–350 g) were used throughout this study and were handled in accordance with the EU guidelines for use of experimental animals. The rats were anesthesized by intraperitoneal injection of urethane (1.5 g/kg) and placed in a head holder in a stereotaxic frame to allow the intracerebroventricular (icv) injection of drugs into the third ventricle (2.5 mm posterior from Bregma and 0.5 lateral to the midline). The rats were divided into four experimental groups: (i) control rats injected with 5 μL saline icv and 200 μL saline ip after 30 min; (ii) LPS-treated rats injected with 5 μL saline icv and 200 μL LPS (200 μg in 200 μL saline) ip after 30 min; (iii) A2AR antagonist-treated rats injected with 5 μL SCH 58261 (50 nM in saline) or 5 μL MSX-3 (1 μM in saline) icv and 200 μL saline ip after 30 min; (iv) LPS + A2AR antagonist-treated rats injected with 5 μL SCH 58261 (50 nM) or 5 μL MSX-3 (1 μM) icv and 200 μL LPS (200 μg) ip after 30 min.

The dose of LPS administered was the same as that previously used in the studies exploring the effect of peripheral administration of LPS on the viability and functionality of hippocampal neurons (e.g. Vereker *et al.* 2000; Kelly *et al.* 2003; Nolan *et al.* 2003). The primary choice of SCH 58261 was based on its sub-nanomolar affinity for A2AR (e.g. Lopes *et al.* 2004) and selectivity towards other adenosine receptors, which is best exemplified by the disappearance of the selective binding of SCH 58261 in A2AR knockout mice (Lopes *et al.* 2004). We selected a concentration of SCH 58261 of 50 nM based on the equivalent effect of this concentration of SCH 58261 (applied through reverse-microdialysis) and ip injection of neuroprotective doses of 0.01–0.1 mg/kg (reviewed in Cunha 2005) on the evoked release of glutamate from rat striatum (cf. Pintor *et al.* 2001; Corsi *et al.* 2003). Likewise, the selected dose of MSX-3 was based on our previous observation that this dose prevented the A2AR-mediated phosphorylation of proteins in the striatum upon cortical stimulation (Quiroz *et al.* 2006, 2009).

Electrophysiological recording of synaptic plasticity in the hippocampus *in vivo*

Three hours after the injection of LPS (or saline) ip, a bipolar concentric stimulation electrode was placed in the perforant pathway (angular bundle, 4.4 mm lateral to lambda) and a recording electrode was positioned in the *stratum moleculare* of the dentate gyrus (2.5 mm lateral and 3.9 mm posterior to bregma), as

previously validated (Vereker *et al.* 2000; Hauss-Wegrzyniak *et al.* 2002; Kelly *et al.* 2003; Nolan *et al.* 2003). The depth of the electrodes was adjusted to obtain potentials with maximal amplitude and the intensity of stimulation was selected to trigger only a single post-synaptic potential. Test shocks were delivered to the perforant path (1 every 30 s) and, after a period to allow stablization of the responses, baseline recordings were taken for 15 min before the experimental protocol to induce LTP was initiated. This consisted of delivery of a tetanic pulse (three trains of stimuli at 250 Hz during 200 ms with an inter-burst interval of 30 s) after which basal stimulation was resumed.

At the end of the electrophysiological recording (i.e. 4 h after the administration of LPS), the rats were killed by decapitation. The hippocampus was rapidly dissected at 4°C, cut in 350 × 350 μm cubes, aliquotted and stored at −20°C as previously described (e.g. Kelly *et al.* 2003) for subsequent biochemical assays.

Quantification of interleukin-1β concentration

The concentration of interleukin-1β (IL-1β) in hippocampal homogenates was assessed by enzyme-linked immunosorbent assay, as previously described (e.g. Vereker *et al.* 2000). Antibody-coated (2.0 μg/mL final concentration, diluted in 0.1 M sodium carbonate buffer, pH 9.5; monoclonal hamster anti-mouse IL-1β antibody) 96-well plates were incubated overnight at 4°C, washed four times with phosphate-buffered saline (PBS) containing 0.05% Tween 20, blocked for 2 h at 37°C with 250 μL of blocking buffer (PBS, pH 7.3, 0.1 M with 4% bovine serum albumin), and incubated with IL-1β standards (100 μL; 0–1000 pg/mL) or samples (supernatants of hippocampal samples homogenized in Krebs solution containing 2 mM $CaCl_2$) for 1 h at 37°C. Samples were incubated with secondary antibody (100 μL; final concentration 0.8 μg/mL in PBS containing 0.05% Tween 20 and 1% bovine serum albumin; biotinylated polyclonal rabbit anti-mouse antibody) for 1 h at 37°C, washed, and incubated in detection agent (100 μL; horseradish peroxidase-conjugated streptavidin; 1 : 1000 dilution in PBS containing 0.05% Tween 20 and 1% bovine serum albumin) and incubated for 15 min at 37°C. 3,3′,5,5′-Tetramethylbenzidine (100 μL; Sigma) was added, samples were incubated at 25°C and absorbance was read at 450 nm within 30 min. Values are expressed as pg IL-1β/mg of protein, quantified as described (Bradford 1976).

Analysis of p38 and JNK phosphorylation

Activation of c-jun N-terminal kinase (JNK) and p38 were quantified by assessing the density of the phosphorylated forms of the kinases using western blot analysis, as previously described (e.g. Vereker *et al.* 2000; Nolan *et al.* 2003). Samples of hippocampal homogenate were solubilized in 5% sodium dodecyl sulfate (SDS) to obtain a protein concentration of 1 mg/mL. Aliquot of homogenate (10 μL) were added to 10 μL of sample buffer (0.5 mM Tris–HCl pH 6.8, 10% glycerol, 10% SDS, 5% β-mercaptoethanol and 0.05% bromophenol blue) and samples were boiled for 5 min. These samples and the pre-stained molecular weight markers (Amersham Pharmacia Biotech, Piscataway, NJ, USA) were separated on SDS gels (10%) and electro-transferred to polyvinylidene difluoride membranes (0.45 μm, from Amersham). After blocking for 2 h at 25°C with 5% milk in Tris-buffered saline [pH 7.6 containing 0.1% Tween 20 (TBS-T)], the membranes were incubated overnight with a mouse antibody against the phosphorylated form of JNK (1 : 2000 dilution, from Santa Cruz Biotechnology, Santa Cruz, CA, USA) or with a mouse antibody against the phosphorylated form of p38 (1 : 300 dilution, from Cell Signaling Technology, Beverly, MA, USA). After four washing periods of 10 min with TBS-T containing 0.5% milk, the membranes were incubated with the alkaline phosphatase-conjugated anti-mouse secondary antibody (1 : 2000 dilution, from Calbiochem, San Diego, CA, USA) in TBS-T containing 1% milk during 90 min at 25°C. After five 10 min washes in TBS-T with 0.5% milk, the membranes were incubated with Enhanced Chemi-Fluorescence for 5 min and then analysed with a VersaDoc 3000 (Bio-Rad Laboratories, Hercules, CA, USA).

The membranes were then re-probed and tested for tubulin immunoreactivity to confirm that similar amounts of protein were applied to the gels. Briefly, the membranes were incubated for 1 h at 25°C with a 0.1 M glycine (pH 7.2) solution and blocked as previously described before incubation with the anti-tubulin antibody (1 : 1000, from Zymed Laboratories Inc., South San Francisco, CA, USA). The membranes were then washed and incubated with alkaline phosphatases-conjugated secondary antibody as previously described.

Analysis of caspase 3 activity

Cleavage of the caspase 3 substrate (Ac-DEVD-AFC peptide, from Alexis Corporation, San Diego, CA, USA) to its fluorescent product was used as a measure of caspase 3 activity, as previously described (Nolan *et al.* 2003). Briefly, slices of hippocampal tissue were washed, homogenized in ice-cold lysis buffer (25 mM HEPES, 5 mM $MgCl_2$, 5 mM EDTA, 5 mM dithiothreitol, 2 mM phenylmethylsufonyl fluoride, 6.25 μg/mL pepstatin A, 6.25 μg/mL aprotinin, pH 7.4) and lysed by cycles of freezing and thawing. Aliquots of these samples (50 μL) were mixed with 50 μL of reaction buffer (50 mM HEPES, 2 mM EDTA, 20% glycerol, 10 mM dithiothreitol, pH 7.4) and 4 μL of caspase 3 substrate (final concentration 10 μM from a stock solution of 250 μM in reaction buffer) and added to 96-well plates. Samples were incubated at 37°C for 60 min in the dark, fluorescence was assessed (excitation 400 nm; emission 505 nm) and enzyme activity was calculated with reference to a standard curve of 7-amino-4-trifluoromethylcoumarin (AFC; 0–10 μM) versus absorbance. The protein concentration of each sample was determined using bovine serum albumin as a standard (Bradford 1976) and values expressed as nmol AFC/mg protein/min.

Immunohistochemical analysis

The detection of microglia-like profiles was carried out as previously described (Cunha *et al.* 2006), using an immunohistochemical detection of OX-42/CD-11b, an epitope which is up-regulated in activated microglia and to a lesser extent in macrophages (e.g. Jensen *et al.* 1997). Four hours (i.e. the same time period used for electrophysiological analysis) after the administration of LPS (200 μg in 200 μL, ip) under urethane anaesthesia, the heart was exposed and after clamping the descending aorta, a catheter was inserted in the ascending aorta. The animal was then perfused with saline with 4% sucrose (200 mL) while opening the right atria to allow the outflow of the perfusate. Rats were then perfused with 200 mL of 4% paraformaldehyde in saline with 4% sucrose. After its fixation, the brain was removed, maintained for 12 h in the same paraformaldehyde solution and subsequently for 48 h in a PBS solution with 30% sucrose. The brain was then frozen in dry ice and

20 μm coronal sections were prepared using a cryostat. The sections were stored in PBS with 0.01% sodium azide until mounting in slides coated with 2% gelatine with chromium and potassium sulphate. The sections were first rinsed for 5 min in PBS and then three times for 5 min with TBS (0.05 M Trizma base buffer containing 150 mM of NaCl, pH 7.2) at room temperature. The slides were blocked with TBS containing 0.2% Triton X-100 and 10% goat serum during 45 min. Sections were incubated in the presence of the mouse anti-CD11b antibody (1 : 200 dilution in TBS containing 0.2% Triton X-100 and 10% normal goat serum, from Serotec, Queluz, Portugal) for 72 h at 4°C, rinsed three times for 10 min in TBS and subsequently incubated with goat anti-mouse secondary antibody conjugated with a fluorophore (Alexa Fluor 488) (1 : 50 dilution in 0.1 M phosphate buffer containing 0.2% Triton X-100 and 10% normal serum) for 2 h at 25°C, then rinsed twice for 10 min in TBS and once for 10 min in distilled water. The sections were dehydrated and passed through xylol before mounting on slides, using Vectashield mounting medium (Vector Laboratories, Burlingame, CA, USA).

Immunohistochemical analysis of phosphorylayed p38 and activated (cleaved) caspase 3 were carried out essentially as previously described (Egeland *et al.* 2010) in 30 μm thick coronal sections from male rats (10 weeks old), killed 4 h after ip injection of LPS (200 μg from a 1 μg/μL solution) or saline. Each series comprised slices 300 μm apart, representative of different hippocampal areas. Immunohistochemistry was performed on free-floating slices and complete series were used for each staining. Slices were blocked in PBS containing 3% bovine serum albumin and 3% Triton X-100 for 1 h at 25°C before incubation in this same solution with the primary antibodies: rabbit anti-phospho-p38 (1 : 100 dilution, from Cell Signaling) or rabbit anti-activated caspase 3 (1 : 300 dilution, from Cell Signaling) together with mouse anti-rat CD11b (1 : 100 dilution, from Serotec) or mouse anti-NeuN (1 : 600 dilution, from Chemicon, Temecula, CA, USA). Excess of antibody was rinsed twice for 10 min with PBS and slices were then incubated for 1 h at 25°C with Alexa Fluor 488 donkey anti-mouse and Alexa Fluor 594 donkey anti-rabbit secondary antibodies (1 : 200 dilution, from Invitrogen, Carlsbad, CA, USA) made up in PBS. Finally, slices were rinsed three times for 10 min in PBS, mounted onto 2% gelatine-subbed microscope slides dried at 25°C and covered with Vectashield Hard Set H-1500 Mounting Medium with DAPI. In the case of double-labelling of phospho-p38 and NeuN, we carried out a sequential incubation with the primary antibody for phospho-p38, then with the respective secondary antibody, followed by incubation with the primary antibody for NeuN and then the respective secondary antibody.

As negative controls, we always tested the labelling in the absence of each primary antibody and in the absence of both primary antibodies, to check for non-specific labelling of the secondary antibodies or cross-reactivity between secondary antibodies. Images were acquired using a Zeiss Axiovert 200 microscope and some images were also acquired with a Zeiss LSM510 META confocal laser-scanning microscope. In the studies attempting to define co-localization of phospho-p38 or cleaved caspase 3 with either NeuN or CD11b, we only carried out a qualitative evaluation of the co-localization rather than a quantification of the actual relative co-localization of both proteins, which would require a considerably larger number of animals.

Analysis of mRNA and protein markers of microglial activation

Quantitative determination of microglial activation in the dentate gyrus of the hippocampus was carried out by western blot quantification of two different markers of microglial activation, namely the CR3/43 protein of the major histocompatibility complex class II and inducible nitric oxide synthase (iNOS). For the four groups of rats (control, treated with LPS, treated with A2AR antagonists or treated with both LPS and A2AR antagonists), animals were killed by decapitation 4 h after the administration of LPS and their hippocampi dissected and sliced (1 mm) to isolate the dentate gyrus.

The dentate gyrus slices from one hippocampus was homogenized and solubilized in 5% SDS, diluted in sample buffer and samples were boiled for 5 min, as described above. These samples (50 μg of protein for CR3/43 or iNOS analyis) and the pre-stained molecular weight markers (Amersham) were analysed by SDS–polyacrylamide gel electrophoresis as described above, using antibodies against CR3/43 (1 : 200 raised in mouse from Santa Cruz Biotechnology) or iNOS/NOS type II (1 : 500, rabbit, BD Transduction Laboratories, Lexington, KY, USA). The membranes were then re-probed and tested for tubulin immunoreactivity to confirm that similar amounts of protein were applied to the gels, as described above.

The dentate gyrus slices from the other hippocampus were used to extract total RNA with a MagNA Lyser Instrument and MagNA Pure Compact RNA Isolation kit (Roche, Amadora, Portugal), according to the manufacturer's instructions. The integrity, quantity and purity of the RNA yields were checked by electrophoresis and spectrophotometry. Reverse transcription for first-strand cDNA synthesis from each sample was performed using random hexamer primer with the Transcriptor First Strand cDNA Synthesis kit (Roche) according to manufacturer's instructions. Resulting cDNAs were used as template for real-time PCR, which was carried out on LightCycler instrument (Roche) using the FastStart DNA Master SYBR Green I kit (Roche). The A2AR and CD11b mRNA expression was calculated relative to β-actin mRNA expression. The following primers (obtained from Tib MolBiol, Berlin, Germany) were used: A2AR (forward: 5′-AGT CAG AAA GAC GGG AAC-3′; reverse: 5′- CAG TAA CAC GAA CGC AA-3′), CD11b (forward: 5′-GAT GCT TAC TTG GGT TAT GCT T-3′; reverse: 5′-CGA GGT GCC CCT AAA ACC A-3′) and β-actin (forward: 5′-AAG TCC CTC ACC CTC CCA AAA G-3′; reverse: 5′-AAG CAA TGC TGT CAC CTT CCC-3′). Quantification was carried out based on standard curves run simultaneously with the test samples, with A2AR, CD11b and β-actin standards being generated by conventional PCR amplification, as previously described (Duarte *et al.* 2007). The PCR products were run in a 3% agarose gel electrophoresis to verify fragment size and the absence of other contaminating fragments, samples were quantified by 260 nm absorbance, and serially diluted to produce the standard curve (100–108 copies/μL). Each real-time PCR reaction was run in triplicate and contained 2 μL of cDNA template, 0.3 μM of each primer, and 3.5 mM $MgCl_2$ in a reaction volume of 20 μL. Cycling parameters were: 95°C for 10 min to activate DNA polymerase, followed by 40–45 cycles at 95°C for 10 s, annealing temperature of 60°C for 10 s, and a final extension step at 72°C for 10 s, in which fluorescence was acquired. The purity and specificity of the resulting PCR products were assessed by melting curve analysis and

electrophoresis. Control reactions were performed to verify that no amplification occurred without cDNA.

Statistical analysis

Values are presented as mean ± SEM of n experiments. Either a Student's t-test for independent means or a one-way analysis of variance (ANOVA) followed by *post hoc* Newmann–Keuls test was used to define statistical differences between values, which were considered significant at $p < 0.05$.

Results

A_{2A} receptor blockade prevents the LPS-induced depression of synaptic plasticity

We report that ip administration of LPS (200 μg in 200 μL) depressed LTP in perforant path-granule cell synapses *in vivo* confirming results of previous studies (see Vereker *et al.* 2000; Hauss-Wegrzyniak *et al.* 2002; Kelly *et al.* 2003). In control rats, which received vehicle alone, the mean percentage change in the slope of the population excitatory post-synaptic potentials (EPSP), measured 30 min after the high frequency train (compared with the EPSP slope in the 5 min immediately prior to tetanic stimulation) was 111.5 ± 0.7% ($n = 5$; $p < 0.05$). However, in rats injected with LPS, the corresponding mean percentage change in population EPSP slope was 102.5 ± 0.8% ($n = 5$); thus LTP was not sustained in these rats (Fig. 1).

The icv administration of the selective antagonist of A2AR, SCH 58261 (5 μL of a 50 nM solution), did not significantly modify ($p > 0.05$) LTP in the dentate gyrus, when compared with control rats (Fig. 1); the mean percentage change in EPSP slope 30 min following tetanic stimulation was 115.2 ± 0.9% ($n = 5$, $p < 0.05$). However, icv administration of SCH 58261 completely prevented the LPS-induced depression of synaptic plasticity in the dentate gyrus (Fig. 1); the mean percentage change in mean EPSP slope 30 min after tetanic stimulation was 113.4 ± 0.4% ($n = 5$), a value which is not significantly different ($p > 0.05$) from that found in control rats but significantly larger ($p < 0.05$) than that observed in rats injected only with LPS.

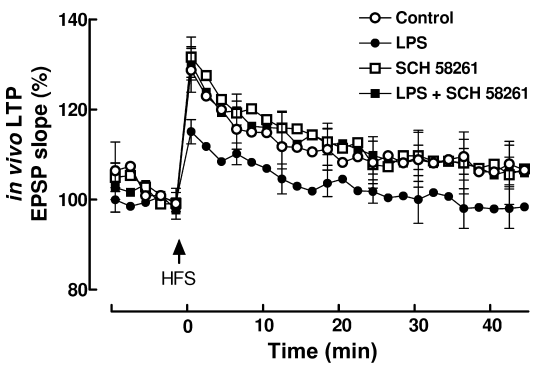

Fig. 1 Effect of lipopolysaccharide (LPS) and/or the selective antagonist of adenosine A_{2A} receptors, SCH 58261, on long-term potentiation (LTP) measured in the rat dentate gyrus *in vivo*. The ordinates represent the slope of the excitatory post-synaptic potentials (EPSPs) recorded in the cell body region of the dentate gyrus after stimulation of the perforant pathway at a frequency of 0.033 Hz in control (open circles), SCH 58261-treated (open squares), LPS-treated (filled circles) or LPS- and SCH 58261-co-treated (filled squares) rats. The arrow indicates the period of application of a high frequency stimulation period (three trains of stimuli at a frequency of 250 Hz during 200 ms with an inter-burst interval of 30 s). Each point represents the mean ± SEM of four experiments.

A_{2A} receptor blockade prevents the LPS-induced biochemical modifications

Previous studies by our group have suggested that the LPS-induced increase in hippocampal IL-1β and neuronal downstream signalling events (i.e. activation of kinases of the stress pathway) mediate the depression of synaptic plasticity in the dentate gyrus (e.g. Vereker *et al.* 2000; Kelly *et al.* 2003; Nolan *et al.* 2003). Here, we asked whether the ability of SCH 58261 to reverse the LPS-induced impairment in LTP might be paralleled by a similar ability to attenuate the LPS-induced increases in phosphorylation of p38 and JNK and activation of caspase 3.

As shown in Fig. 2(a)–(d), LPS increased the density of the phosphorylated forms of p38 and of JNK in hippocampal tissue to 131 ± 6% and 129 ± 9% of control values, respectively ($n = 5$, $p < 0.05$). Administration of SCH 58261 did not significantly change the density of the phosphorylated forms of p38 or JNK (103 ± 8% and 98 ± 9% of control, respectively; $p > 0.05$ vs. control, $n = 5$), but prevented the LPS-induced increases in both p38 and JNK (100 ± 5% and 98 ± 9% of control; $p < 0.05$ vs. LPS, $n = 5$). Activated MAP kinases play different roles in different cell types in the central nervous system. Thus, we next investigated if the activated form of p38 was located in neurons or in glial cells. As shown in Fig. 2(e), LPS triggered an enhancement of the immunoreactivity of the phosphorylated form of p38 throughout the dentate gyrus ($n = 3$), which was more evident in the stratum moleculare than in the stratum granulosum; more detailed cellular analysis showed that the LPS-induced enhanced immunoreactivity of the phosphorylated form of p38 was mostly co-located with philipodia labelled with a microglia marker (CD11b) in the stratum moleculare (Fig. 2f) than with a neuronal markers (NeuN) in the stratum granulosum (Fig. 2g).

In parallel with the effect of LPS on phosphorylation of JNK and p38, we report a significant increase in the activity of caspase 3 in hippocampal tissue prepared from LPS-treated, compared with control, rats ($n = 5$, $p < 0.05$; Fig. 3a). Administration of SCH 58261 did not significantly change the activity of caspase 3 ($p > 0.05$, $n = 3$), but

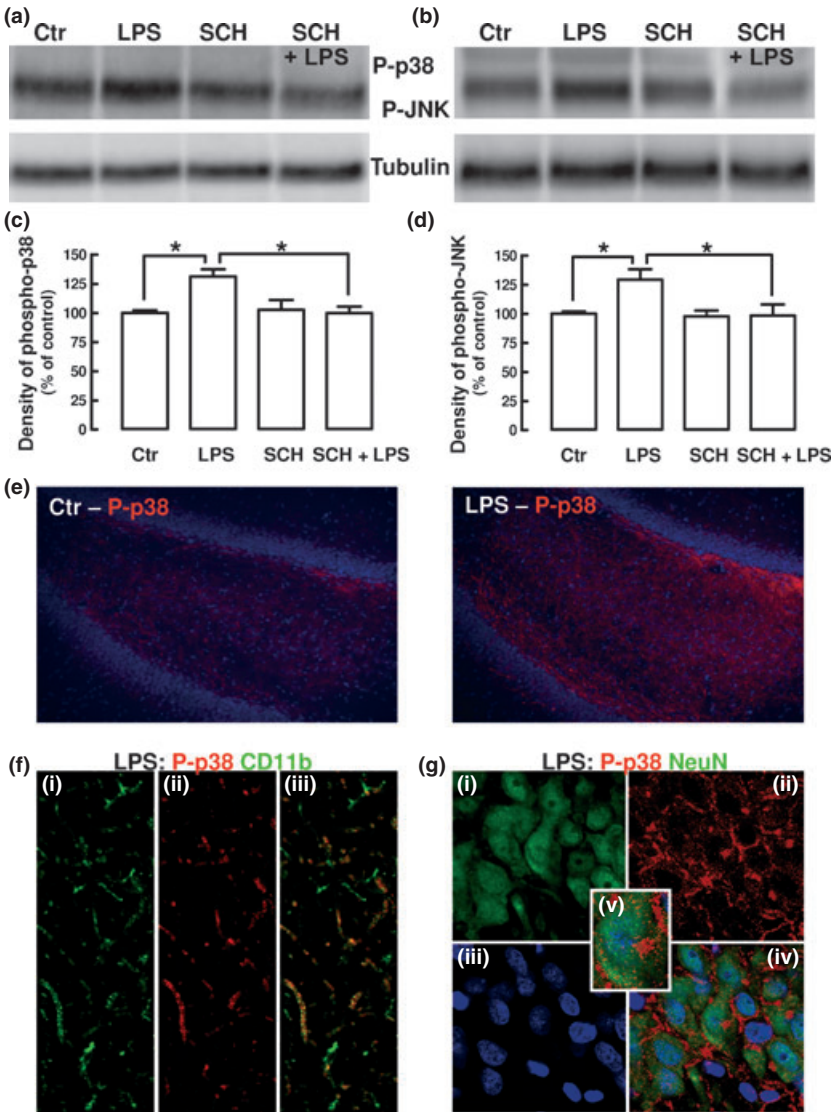

Fig. 2 Effect of lipopolysaccharide (LPS) and/or the selective antagonist of adenosine A_{2A} receptors, SCH 58261, on the density of the phosphorylated forms of two stress activated kinases, p38 (panels a and c) and JNK (panels b and d) in the rat hippocampus. Four hours after drug treatments, the hippocampus of control, SCH 58261-treated, LPS-treated or LPS- and SCH 58261-co-treated rats was dissected and homogenized for western blot analysis. Panels a and b present western blots comparing the density of immunoreactivity of the phosphorylated form of p38 (a) and of JNK (b) in the hippocampus of each group of rats. The re-probing of the same gels against tubulin is displayed below. Panels c and d present the average results (mean ± SEM), obtained in 3–5 experiments, comparing the density of immunoreactivity of the phosphorylated form of p38 (c) and of JNK (d) in the hippocampus of each group of rats. $^*p < 0.05$ between the indicated bars. Immunohistochemical analysis confirmed an enhanced density of phosphorylated p38 immunoreactivity in the dentate gyrus of LPS-treated rats (right photograph of panel e) compared with control (left photograph of panel e). This LPS-induced enhancement of phosphorylated p38 immunoreactivity was mostly co-localized with CD11b, a marker of microglia (panel f: i-CD11b; ii-phosphorylated p38; iii-merging of the previous two photographs), in philopodia located in the stratum moleculare, but was also co-localized with NeuN (neuronal nuclei), a marker of neurons (panel g: i-NeuN; ii-phosphorylated p38; iii-Hoescht 33342, which stains DNA; iv-merging of the previous three photographs; v-amplified single neuronal cell body), in the stratum granulosum. These photographs are representative of immunohistochemical analysis carried out in three LPS-treated rats.

prevented the LPS-induced increase of caspase 3 activity so that there was a significant difference ($p < 0.05$) in the enzyme activity in hippocampal tissue prepared from LPS-treated rats and in tissue prepared from rats which were treated with LPS and SCH 58261 (Fig. 3a). We next attempted to determine which cell type displayed increased

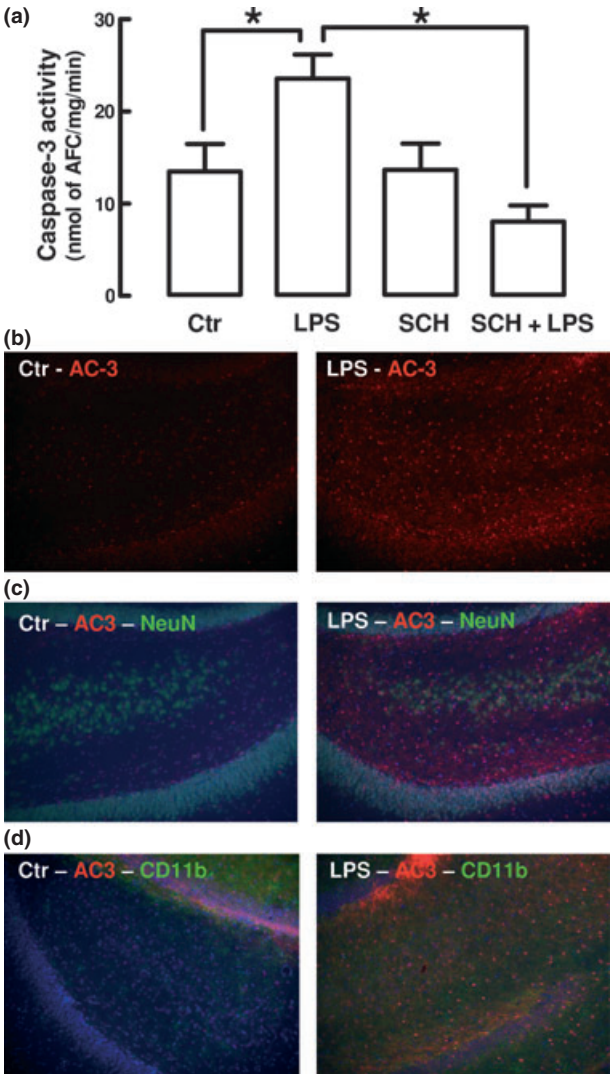

Fig. 3 Effect of lipopolysaccharide (LPS) and/or the selective antagonist of adenosine A_{2A} receptors, SCH 58261, on the activity of caspase 3 in the rat hippocampus. Four hours after drug treatments, the hippocampus of control, SCH 58261-treated, LPS-treated or LPS- and SCH 58261-co-treated rats was dissected and homogenized for determination of the activity of caspase 3 expressed in nmol of 7-amino-4-trifluoromethylcoumarine (AFC), normalized by the concentration of protein in each sample (a). Each bar represents the mean ± SEM of five experiments. $^*p < 0.05$ between the indicated bars. Immunohistochemical analysis confirmed an enhanced density of activated (cleaved) caspase 3 immunoreactivity in the dentate gyrus of LPS-treated rats (right photograph of panel b) compared with control (left photograph of panel b). Panel c displays triple-labelling immunohistocehmical analysis of cleaved caspase 3 (red), the neuronal marker (NeuN, green) and Hoescht 33342-labelled nuclei (blue) in control (left photograph) and LPS-treated rats (right photograph) showing that cleaved caspase 3 was not was not co-localized with NeuN immunoreactivity. Panel d displays triple-labelling immunohistocehmical analysis of cleaved caspase 3 (red), the microglia marker (CD11b, green) and Hoescht 33342-labelled nuclei (blue) in control (left photograph) and LPS-treated rats (right photograph) showing that cleaved caspase 3 was instead co-localized with CD11b immunoreactivity. These photographs are representative of immunohistochemical analysis carried out in three LPS-treated rats.

activity of caspase 3 in the dentate gyrus. Immunohistochemical analysis revealed that LPS caused a scattered increase of activated (cleaved) caspase 3 in the dentate gyrus (Fig. 3b), which was not co-localized with neuronal markers (NeuN, Fig. 3c) but rather with a microglia marker (CD11b, Fig. 3d).

A_{2A} receptor blockade prevents the LPS-induced neuroinflammation

The observed protective effect of the tested A2AR antagonist against LPS-induced inhibition of LTP might either result from the ability of neuronal A2AR to control the effects of inflammatory mediators on neurons or result from the ability of A2AR to control the reactivity of microglia and the consequent generation of inflammatory mediators. Thus, we next tested if the blockade of A2AR could control activation of microglia and the previously described LPS-induced increase in IL-1β (see Vereker *et al.* 2000).

The identification of microglial cells was carried out by immunohistochemical detection of anti-CD11b, a validated marker of activated microglia cells (Jensen *et al.* 1997). As presented in Fig. 4, we can conclude that 4 h after administration of LPS, there is an increase in the number of elements labelled with the anti-CD11b antibody (compare panels A and C from Fig. 4). Furthermore, the labelled profiles displayed a more intense immunoreactivity and a morphology characteristic of early activated microglia *in situ*, that is, enlarged cell body with short and thick processes (Fig. 4c) (e.g. Jensen *et al.* 1997). Administration of SCH 58261 did not modify the profile of CD11b immunoreactivity compared with control ($n = 4$; Fig. 4b), but prevented the LPS-induced changes in CD11b immunoreactivity ($n = 4$; Fig. 4d).

Accordingly, 4 h after the administration of LPS, there was an increase in the density of markers of microglia activation, such as the major histocompatibility complex class II protein CR3/43 ($n = 7$, Fig. 5a) and iNOS ($n = 7$, Fig. 5b). The administration of either SCH 58261 or another selective A2AR antagonist, MSX-3, did not modify the density of each of these microglia markers, but prevented the LPS-induced changes in both CR3/43 ($n = 3$–4, Fig. 5a) and iNOS ($n = 3$–4, Fig. 5b). Further linking the control by A2AR of microglia activation, we report a parallel increase in the expression of both CD11b ($n = 7$; Fig. 5c) and A2AR mRNA ($n = 7$, Fig. 5d) in the hippocampus measured 4 h after the administration of LPS.

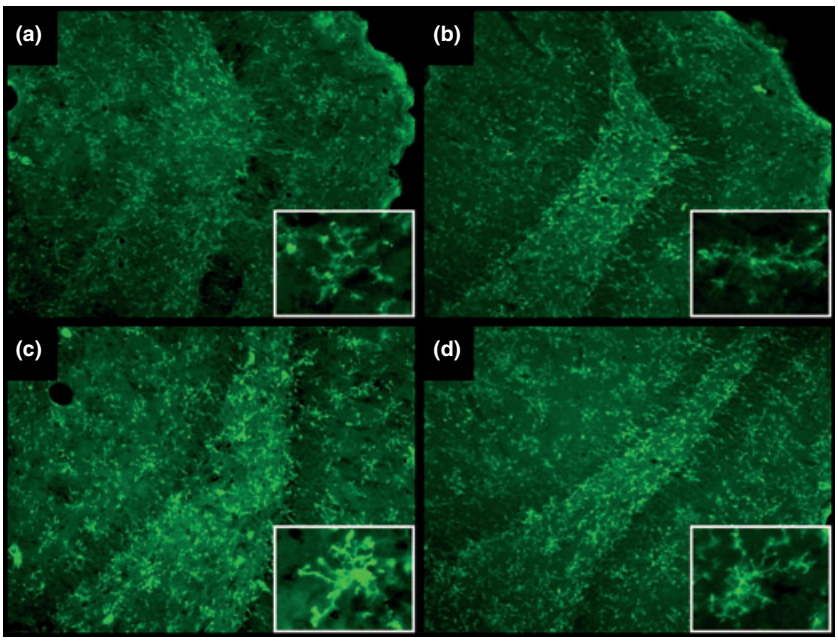

Fig. 4 Effect of lipopolysaccharide (LPS) and/or the selective antagonist of adenosine A_{2A} receptors, SCH 58261, on the appearance of reactive microglia in the rat dentate gyrus. Four hours after the drug treatments, control (a), SCH 58261-treated (b), LPS-treated (c) or LPS- and SCH 58261-co-treated (d) rats were perfused with paraformaldehyde for fixation of the brain, which was sliced (20 μm). The coronal sections were labelled by immunohistochemistry using a mouse anti-CD11b antibody (a marker of activated microglial cells) and a goat anti-mouse secondary antibody labelled with Alexa Fluor 488. The insert figures in each panels display the pattern of labelling and morphology of a single microglia cell, obtained from the presented picture, at higher magnification. The pictures presented are representative of 3–4 experiments with qualitatively similar results.

In accordance with a direct ability of A2AR to control microglia activation, we found that LPS treatment caused a significant increase in hippocampal concentration of IL-1β ($n = 5$, $p < 0.05$; Fig. 6). Administration of SCH 58261 alone did not significantly change ($p > 0.05$, $n = 3$) IL-1β concentration, but prevented the LPS-induced increase in IL-1β ($n = 3$, $p < 0.05$; Fig. 6).

Discussion

The main conclusion from this study is that the blockade of adenosine A2AR prevents the induction of a neuroinflammatory situation triggered by LPS and the consequent biochemical modifications and neuronal dysfunction in the hippocampus.

Several previous studies have already studied the cascade of events that lead to neuronal dysfunction after the administration of LPS and the consequent neuronal damage, particularly in the hippocampus (Vereker *et al.* 2000; Hauss-Wegrzyniak *et al.* 2002; Kelly *et al.* 2003; Nolan *et al.* 2003). Thus, LPS triggers an increase in the concentration of the pro-inflammatory cytokine IL-1β, which plays a key role in triggering neuronal dysfunction (Vereker *et al.* 2000; reviewed in Allan *et al.* 2005). The precise mechanism by which peripherally administered LPS triggers neuroinflammation still remains to be defined but is thought to involve the activation of microglial cells (Kim *et al.* 2000), independent of systemic inflammation (Chakravarty and Herkenham 2005). In response to a neuroinflammatory situation, neurons react by up-regulating activation of the stress kinases p38 and JNK, which negatively impact on synaptic function leading to depression of LTP in dentate gyrus (Kelly *et al.* 2003; Nolan *et al.* 2003). In parallel, Poly-ADP ribose polymerase cleavage and activation of caspase 3 are up-regulated leading to a delayed LPS-induced neuronal cell death (Hauss-Wegrzyniak *et al.* 2002; Nolan *et al.* 2003). In the present study, we observed that the blockade of A2AR, using its selective antagonist SCH 58261 (see Fredholm *et al.* 2005), prevented the principal modifications caused by LPS that are associated with the LPS-induced neuroinflammation and neuronal dysfunction. Thus, the administration of SCH 58261 prevented the ability of LPS to increase the phosphorylation of p38 and of JNK, as well the activation of caspase 3, and also prevented the LPS-induced depression of LTP. This ability of SCH 58261 to prevent LPS-induced LTP depression is unlikely to be a direct synaptic effect of the A2AR antagonist (although this cannot be excluded), because this A2AR antagonists has previously been shown to inhibit rather than to increase LTP at other hippocampal synapses (Costenla *et al.* 2008; Rebola *et al.* 2008). It is

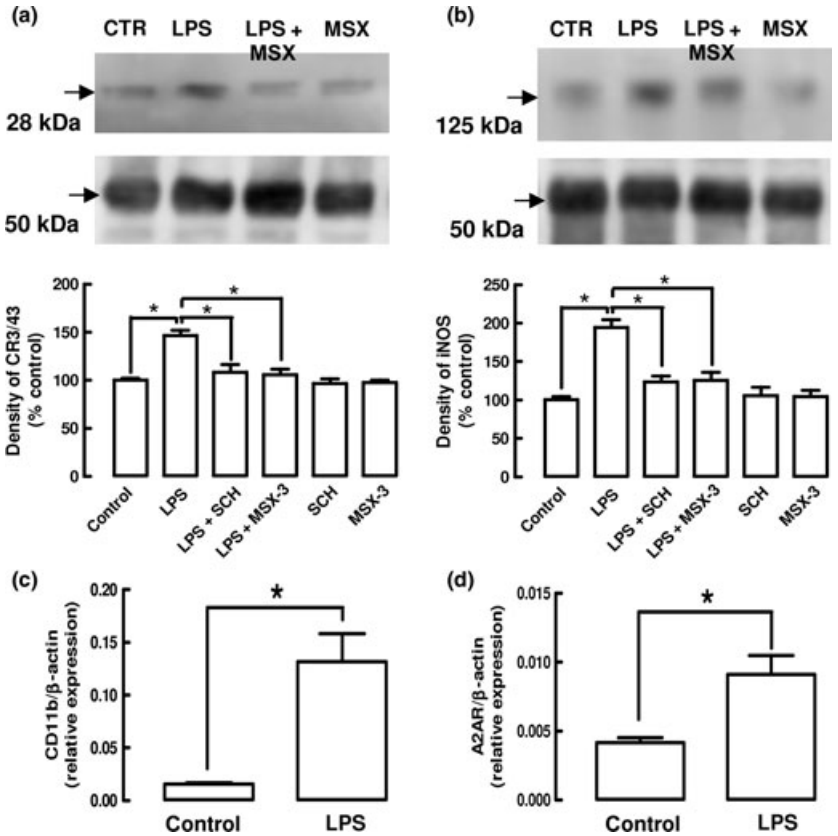

Fig. 5 Effect of lipopolysaccharide (LPS) and/or the selective antagonists of adenosine A_{2A} receptors, SCH 58261 or MSX-3, on the expression and density of markers of microglia activation. Four hours after drug treatments, control, SCH 58261-treated, LPS-treated or LPS- and SCH 58261 or MSX-3-co-treated rats were killed, one hippocampus being used for western blot analysis and the other for real-time PCR analysis. Panels a and b present western blots comparing the density of immunoreactivity of the major histocompatibility complex class II (MHC-II) protein CR3/43 (a) and iNOS (b) in the hippocampus of each group of rats. The re-probing of the same gels against tubulin is displayed below. The graph bars below present the average results (mean ± SEM), obtained in 3–4 experiments, comparing the density of immunoreactivity of the two markers of microglia activation; $^*p < 0.05$ between the indicated bars. Panel c and d display the expression of CD11b (c) and A2AR (d) 4 h after drug treatment. CD11b and A2AR mRNA levels (copies/μL) were determined with QRT-PCR and normalized to the level of β-actin mRNA. Bars represent mean ± SEM from seven different rats, run in triplicate; $^*p < 0.05$ between bars.

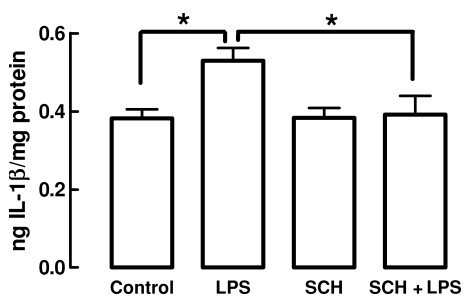

Fig. 6 Effect of lipopolysaccharide (LPS) and/or the selective antagonist of adenosine A_{2A} receptors, SCH 58261, on the levels of interleukin-1β in the rat hippocampus. Four hours after drug treatments the hippocampus of control, SCH 58261-treated, LPS-treated or LPS- and SCH 58261-co-treated rats was dissected and homogenized for analysis by ELISA of interleukin-1β (IL-1β) levels. Each bar represents the mean ± SEM of 5 experiments. $^*p < 0.05$ between the indicated bars.

important to note that, in the absence of LPS, SCH 58261 was devoid of effects in any of these properties. It is therefore concluded that the blockade of A2AR conferred a robust protection in this model of neuroinflammation, as observed in other *in vivo* models of brain neurotoxicity (reviewed in Cunha 2005; Chen *et al.* 2007).

Here, we also report that blockade of A2AR also decreased the extent of neuroinflammation caused by LPS. This was concluded by simultaneous ability of A2AR blockade to prevent the LPS-induced recruitment and activation of microglia and the increase in IL-1β levels, a master regulator of neuroinflammation that contributes to neurodegeneration (Allan *et al.* 2005). Furthermore, the observed ability of A2AR to prevent biochemical changes, such as increased phopshorylated form of p38 and increased cleaved caspase 3, that we found to be associated with microglia dynamics (see Wirenfeldt *et al.* 2007; Ohnishi

et al. 2010) further argues for a direct ability of A2AR on microglia cells to control LPS-induced neuroinflammation. However, it remains to be determined if the A2AR mainly control the chemotaxis or the activation of microglial cells. This might require analysis *in vivo*, because there is a notable difference between the impact of A2AR on microglia reactivity *in vivo* (present results, see also Pierri *et al.* 2005; Melani *et al.* 2006; Minghetti *et al.* 2007; Yu *et al.* 2008) and in purified microglial cells in culture (Orr *et al.* 2009; van der Putten *et al.* 2009; Dai *et al.* 2010). It is likely that other factors or cell types in the brain parenchyma may play a crucial role in formatting the pattern of A2AR-mediated control of microglial reactivity (see Saura *et al.* 2005; Dai *et al.* 2010). Furthermore, the role of A2AR in controlling neuroinflammation may also depend on the cell types involved in supporting brain inflammation. In fact, it is notable that in experimental situations associated with disruption of the blood brain barrier and invasion of the brain by peripheral inflammatory cells, such as brain hemorrhage (Mayne *et al.* 2001) or prolonged stenosis (Duan *et al.* 2009), it is the activation rather than the blockade of A2AR that control neuroinflammation. However, when resident microglia trigger and sustain neuroinflammation, such as in early periods after LPS administration (see Chakravarty and Herkenham 2005), our results indicate that it is the blockade of A2AR that controls neuroinflammation. These results are in agreement with a recent report describing the ability of chronic caffeine consumption (an antagonist of adenosine receptors) to control neuroinflammation (Brothers *et al.* 2010) and experimental autoimmune encephalomyelitis (Chen *et al.* 2010).

A question that still remains to be resolved is the identity of the cell type in which A2AR are located that mounts the neuroinflammatory response. A previous study concluded that in was A2AR located in bone marrow cells infiltrating in the brain parenchyma that were responsible for the control of cortical infarct after middle cerebral artery occlusion, while blockade of A2AR on brain resident A2AR only accounted for 20% of observed neuroprotection (Yu *et al.* 2004). However, ischemic brain injury causes an extensive disruption of the blood-brain barrier and consequent massive invasion of peripheral lymphoid cells, far greater that than occurring in other neurodegenerative conditions (reviewed in Ballabh *et al.* 2004). Accordingly, in another similar study using a model of Parkinson's disease based on MPTP intoxication, we found that it was non-neuronal brain resident A2AR that contributed for neuroprotection, rather than infiltrating bone marrow-derived cells; this was based on the combined use of forebrain neuronal-selective A2AR knockout mice and bone marrow transplants after bone marrow destruction by γ-irradiation (Yu *et al.* 2008). Given that the neuroinflammation triggered by intraperitoneal administration of LPS requires a response from CNS-resident cells independent of systemic cytokine effects (Chakravarty and Herkenham 2005), it is most likely that it is A2AR present in microglia (Saura *et al.* 2005) or astrocytes (Nishizaki *et al.* 2002) that play a role in the control of LPS-induced neuroinflammation. The currently observed parallel increase in the expression of A2AR, together with markers of microglial activation in brain tissue, also observed by others in cultured cells (van der Putten *et al.* 2009) and upon different brain insults (Trincavelli *et al.* 2008; Yu *et al.* 2008), further strengthens the hypothesis that it may be A2AR in resident microglia cells that control neuroinflammation in conditions where the invasion of the brain parenchyma by peripheral inflammatory cells is limited.

This observed ability of A2AR to control microglial recruitment and activation and the increase in brain levels of IL-1β prompts the hypothesis that the A2AR-mediated control of the genesis of neuroinflammatory processes in pathological conditions may play an important hitherto unrecognized role in the neuroprotective effect afforded by A2AR blockade. This does not rule out the possibility that A2AR located in neurons (e.g. Rebola *et al.* 2005) may also contribute to the control of neurodegeneration (see Dall'Igna *et al.* 2003; Mojsilovic-Petrovic *et al.* 2006; Silva *et al.* 2007; Stone and Behan 2007; Canas *et al.* 2009). However, it is important to note that the blockade of A2AR is particularly effective when tested *in vivo*. In fact, blockade of A2AR affords a more robust neuroprotection in hippocampal regions upon *in vivo* ischemia (e.g. Chen *et al.* 1999) when compared with the effect found upon chemical ischemia in hippocampal slices *in vitro* (Latini *et al.* 1999; Higashi *et al.* 2002). This argues that mechanisms other than a direct neuronal protection, such as the control of neuroinflammation, might be prominent in the neuroprotection afforded by A2AR blockade.

Thus, the present study provides evidence to support the hypothesis that blockade of A2AR abrogates the LPS-induced neuroinflammation and the consequent neuronal dysfunction in the hippocampus caused by the LPS-induced neuroinflammation. These observations support the hypothesis that the control of neuroinflammation by A2AR might be a common mechanism underlying the robust neuroprotection afforded by antagonists of A2AR against a diversity of neurodegenerative conditions which involve neuroinflammation, such as epilepsy, Alzheimer's or Parkinson's disease.

Acknowledgements

We are in debt to Andrea Theman, João M.N. Duarte and Daniela Pochmann for their help in some experiments, for the assistance of Luisa Cortes in obtaining the confocal microscopy images and for the dedicated and competent help of Alexandre Pires to handle the animals. We thank Sergi Ferré for providing an aliquot of MSX-3, Per Svenningsson for his generous guidance in the immunohistochemical protocols and Jiang-Fan Chen for the fruitful discussions on the mechanisms of adenosine neuroprotection over the years.

This study was supported by Fundação para a Ciência e para a Tecnologia and by a joint Portuguese-Brazilian grant (CAPES-GRICES). Claire Barry is funded by the Health Research Board, Ireland.

References

Allan S. N., Tyrrell P. J. and Rothwell N. J. (2005) Interleukin-1 and neuronal injury. *Nat. Rev. Immunol.* **5**, 629–640.

Ballabh P., Braun A. and Nedergaard M. (2004) The blood-brain barrier: an overview: structure, regulation, and clinical implications. *Neurobiol. Dis.* **16**, 1–13.

Bradford M. M. (1976) A rapid and sensitive method for the quantification of microgram quantities of protein utilizing the principle of protein-dye binding. *Anal. Biochem.* **72**, 248–254.

Brothers H. M., Marchalant Y. and Wenk G. L. (2010) Caffeine attenuates lipopolysaccharide-induced neuroinflammation. *Neurosci. Lett.* **480**, 97–100.

Canas P. M., Porciúncula L. O., Cunha G. M. A., Silva C. G., Machado N. J., Oliveira J. M. A., Oliveira C. R. and Cunha R. A. (2009) Adenosine A2A receptor blockade prevents synaptotoxicity and memory dysfunction caused by β-amyloid peptides via p38 mitogen-activated protein kinase pathway. *J. Neurosci.* **29**, 14741–14751.

Chakravarty S. and Herkenham M. (2005) Toll-like receptor 4 on nonhematopoietic cells sustains CNS inflammation during endotoxemia, independent of systemic cytokines. *J. Neurosci.* **25**, 1788–1796.

Chen J. F., Huang Z., Ma J., Zhu J., Moratalla R., Standaert D., Moskowitz M. A., Fink J. S. and Schwarzschild M. A. (1999) A_{2A} adenosine receptor deficiency attenuates brain injury induced by transient focal ischemia in mice. *J. Neurosci.* **19**, 9192–9200.

Chen J. F., Sonsalla P. K., Pedata F., Melani A., Domenici M. R., Popoli P., Geiger J. D., Lopes L. V. and de Mendonça A. (2007) Adenosine A_{2A} receptors and brain injury: broad spectrum of neuroprotection, multifaceted actions and "fine tuning" modulation. *Prog. Neurobiol.* **83**, 310–331.

Chen G. Q., Chen Y. Y., Wang X. S., Wu S. Z., Yang H. M., Xu H. Q., He J. C., Wang X. T., Chen J. F. and Zheng R. Y. (2010) Chronic caffeine treatment attenuates experimental autoimmune encephalomyelitis induced by guinea pig spinal cord homogenates in Wistar rats. *Brain Res.* **1309**, 116–125.

Corsi C., Pinna A., Gianfriddo M., Melani A., Morelli M. and Pedata F. (2003) Adenosine A_{2A} receptor antagonism increases striatal glutamate outflow in dopamine-denervated rats. *Eur. J. Pharmacol.* **464**, 33–38.

Costenla A. R., Diógenes M. J., Ribeiro J. A., Cunha R. A. and de Mendonça A. (2008) Enhanced role of adenosine A_{2A} receptors on long-term potentiation in the rat hippocampus upon aging. *Soc. Neurosci.* 541.18.

Cunha R. A. (2005) Neuroprotection by adenosine in the brain: from A_1 receptor activation to A_{2A} receptor blockade. *Purinergic Signal.* **1**, 111–134.

Cunha G. M. A., Canas P. M., Oliveira C. R. and Cunha R. A. (2006) Increased density and synapto-protective effect of adenosine A_{2A} receptors upon sub-chronic restraint stress. *Neuroscience* **141**, 1775–1781.

Dai S. S., Zhou Y. G., Li W. *et al.* (2010) Local glutamate level dictates adenosine A_{2A} receptor regulation of neuroinflammation and traumatic brain injury. *J. Neurosci.* **30**, 5802–5810.

Dall'Igna O. P., Porciúncula L. O., Souza D. O., Cunha R. A. and Lara D. R. (2003) Neuroprotection by caffeine and adenosine A_{2A} receptor blockade of β-amyloid neurotoxicity. *Br. J. Pharmacol.* **138**, 1207–1209.

Duan W., Gui L., Zhou Z., Liu Y., Tian H., Chen J. F. and Zheng J. (2009) Adenosine A_{2A} receptor deficiency exacerbates white matter lesions and cognitive deficits induced by chronic cerebral hypoperfusion in mice. *J. Neurol. Sci.* **285**, 39–45.

Duarte J. M., Nogueira C., Mackie K., Oliveira C. R., Cunha R. A. and Köfalvi A. (2007) Increase of cannabinoid CB1 receptor density in the hippocampus of streptozotocin-induced diabetic rats. *Exp. Neurol.* **204**, 479–484.

Egeland M., Warner-Schmidt J., Greengard P. and Svenningsson P.. (2010) Neurogenic effects of fluoxetine are attenuated in p11 (S100A10) knockout mice. *Biol. Psychiatry* **67**, 1048–1056.

Fredholm B. B., Chen J. F., Cunha R. A., Svenningsson P. and Vaugeois J. M. (2005) Adenosine and brain function. *Int. Rev. Neurobiol.* **63**, 191–270.

Hauss-Wegrzyniak B., Lynch M. A., Vraniak P. D. and Wenk G. L. (2002) Chronic brain inflammation results in cell loss in the entorhinal cortex and impaired LTP in perforant path-granule cell synapses. *Exp. Neurol.* **176**, 336–341.

Higashi H., Meno J. R., Marwaha A. S. and Winn H. R. (2002) Hippocampal injury and neurobehavioral deficits following hyperglycemic cerebral ischemia: effect of theophylline and ZM 241385. *J. Neurosurg.* **96**, 117–126.

Jensen M. B., Finsen B. and Zimmer J. (1997) Morphological and immunophenotypic microglial changes in denervated fascia dentate of adult rats: correlation with blood brain barrier damage and astroglial reactions. *Exp. Neurol.* **143**, 103–106.

Kelly A., Vereker E., Nolan Y., Brady M., Barry C., Loscher C. E., Mills K. H. and Lynch M. A. (2003) Activation of p38 plays a pivotal role in the inhibitory effect of lipopolysaccharide and interleukin-1beta on long-term potentiation in rat dentate gyrus. *J. Biol. Chem.* **278**, 19453–19462.

Kim W. G., Mohney R. P., Wilson B., Jeohn G. H., Liu B. and Hong J. S. (2000) Regional difference in susceptibility to lipopolysaccharide-induced neurotoxicity: role of microglia. *J. Neurosci.* **20**, 6309–6316.

Kreutzberg G. W. (1996) Microglia: a sensor for pathological events in the CNS. *Trends Neurosci.* **19**, 312–318.

Latini S., Bordoni F., Corradetti R., Pepeu G. and Pedata F. (1999) Effect of A_{2A} adenosine receptor stimulation and antagonism on synaptic depression induced by in vitro ischaemia in rat hippocampal slices. *Br. J. Pharmacol.* **128**, 1035–1044.

Lopes L. V., Halldner L., Rebola N., Johansson B., Ledent C., Chen J. F., Fredholm B. B. and Cunha R. A. (2004) Binding of the prototypical adenosine A_{2A} receptor agonist, CGS 21680, to the cerebral cortex of adenosine A_1 and A_{2A} receptor knockout mice. *Br. J. Pharmacol.* **141**, 1006–1014.

Marchetti B. and Abbracchio M. P. (2005) To be or not to be (inflamed) – is that the question in anti-inflammatory drug therapy of neurodegenerative disorders? *Trends Pharmacol. Sci.* **26**, 517–525.

Mayne M., Fotheringham J., Yan H. J., Power C., Del Bigio M. R., Peeling J. and Geiger J. D. (2001) Adenosine A_{2A} receptor activation reduces proinflammatory events and decreases cell death following intracerebral hemorrhage. *Ann. Neurol.* **49**, 727–735.

Melani A., Gianfriddo M., Vannucchi M. G., Cipriani S., Baraldi P. G., Giovannini M. G. and Pedata F. (2006) The selective A_{2A} receptor antagonist SCH 58261 protects from neurological deficit, brain damage and activation of p38 MAPK in rat focal cerebral ischemia. *Brain Res.* **1073–1074**, 470–480.

Minghetti L., Greco A., Potenza R. L., Pezzola A., Blum D., Bantubungi K. and Popoli P. (2007) Effects of the adenosine A_{2A} receptor antagonist SCH 58621 on cyclooxygenase-2 expression, glial activation, and brain-derived neurotrophic factor availability in a

rat model of striatal neurodegeneration. *J. Neuropathol. Exp. Neurol.* **66**, 363–371.

Mojsilovic-Petrovic J., Jeong G. B., Crocker A., Arneja A., David S., Russell D. and Kalb R. G.. (2006) Protecting motor neurons from toxic insult by antagonism of adenosine A_{2a} and Trk receptors. *J. Neurosci.* **26**, 9250–9263.

Nishizaki T., Nagai K., Nomura T. *et al.* (2002) A new neuromodulatory pathway with a glial contribution mediated via A_{2a} adenosine receptors. *Glia* **39**, 133–147.

Nolan Y., Vereker E., Lynch A. M. and Lynch M. A. (2003) Evidence that lipopolysaccharide-induced cell death is mediated by accumulation of reactive oxygen species and activation of p38 in rat cortex and hippocampus. *Exp. Neurol.* **184**, 794–804.

Ohnishi M., Katsuki H., Izumi Y., Kume T., Takada-Takatori Y. and Akaike A. (2010) Mitogen-activated protein kinases support survival of activated microglia that mediate thrombin-induced striatal injury in organotypic slice culture. *J. Neurosci. Res.* **88**, 2155–2164.

Olesen J. and Leonardi M. (2003) The burden of brain diseases in Europe. *Eur. J. Neurol.* **10**, 471–477.

Orr A. G., Orr A. L., Li X. J., Gross R. E. and Traynelis S. F. (2009) Adenosine A_{2A} receptor mediates microglial process retraction. *Nat. Neurosci.* **12**, 872–878.

Pierri M., Vaudano E., Sager T. and Englund U. (2005) KW-6002 protects from MPTP induced dopaminergic toxicity in the mouse. *Neuropharmacology* **48**, 517–524.

Pintor A., Quarta D., Pèzzola A., Reggio R. and Popoli P. (2001) SCH 58261 (an adenosine A_{2A} receptor antagonist) reduces, only at low doses, K^+-evoked glutamate release in the striatum. *Eur. J. Pharmacol.* **421**, 177–180.

van der Putten C., Zuiderwijk-Sick E. A., van Straalen L., de Geus E. D., Boven L. A., Kondova I., IJzerman A. P. and Bajramovic J. J. (2009) Differential expression of adenosine A_3 receptors controls adenosine A_{2A} receptor-mediated inhibition of TLR responses in microglia. *J. Immunol.* **182**, 7603–7612.

Quiroz C., Gomes C., Pak A. C., Ribeiro J. A., Goldberg S. R., Hope B. T. and Ferré S. (2006) Blockade of adenosine A_{2A} receptors prevents protein phosphorylation in the striatum induced by cortical stimulation. *J. Neurosci.* **26**, 10808–10812.

Quiroz C., Luján R., Uchigashima M. *et al.* (2009) Key modulatory role of presynaptic adenosine A_{2A} receptors in cortical neurotransmission to the striatal direct pathway. *Sci.World J.* **9**, 1321–1344.

Rebola N., Canas P. M., Oliveira C. R. and Cunha R. A. (2005) Different synaptic and subsynaptic localization of adenosine A_{2A} receptors in the hippocampus and striatum of the rat. *Neuroscience* **132**, 893–903.

Rebola N., Lujan R., Cunha R. A. and Mulle C. (2008) Adenosine A_{2A} receptors are essential for long-term potentiation of NMDA-EPSCs at hippocampal mossy fiber synapses. *Neuron* **57**, 121–134.

Saura J., Angulo E., Ejarque A. *et al.* (2005) Adenosine A_{2A} receptor stimulation potentiates nitric oxide release by activated microglia. *J. Neurochem.* **95**, 919–929.

Silva C. G., Porciúncula L. O., Canas P. M., Oliveira C. R. and Cunha R. A. (2007) Blockade of adenosine A2A receptors prevents staurosporine-induced apoptosis of rat hippocampal neurons. *Neurobiol. Dis.* **27**, 182–189.

Sitkovsky M. V. and Ohta A. (2005) The 'danger' sensor that stop the immune response: the A_2 adenosine receptors? *Trends Immunol.* **26**, 299–304.

Stone T. W. and Behan W. M. (2007) Interleukin-1beta but not tumor necrosis factor-alpha potentiates neuronal damage by quinolinic acid: protection by an adenosine A_{2A} receptor antagonist. *J. Neurosci. Res.* **85**, 1077–1085.

Trincavelli M. L., Melani A., Guidi S., Cuboni S., Cipriani S., Pedata F. and Martini C. (2008) Regulation of A_{2A} adenosine receptor expression and functioning following permanent focal ischemia in rat brain. *J. Neurochem.* **104**, 479–490.

Vereker E., Campbell V., Roche E., McEntee E. and Lynch M. A. (2000) Lipopolysaccharide inhibits long term potentiation in the rat dentate gyrus by activating caspase-1. *J. Biol. Chem.* **275**, 26252–26258.

Wirenfeldt M., Dissing-Olesen L., Anne Babcock A., Nielsen M., Meldgaard M., Zimmer J., Azcoitia I., Leslie R. G., Dagnaes-Hansen F. and Finsen B. (2007) Population control of resident and immigrant microglia by mitosis and apoptosis. *Am. J. Pathol.* **171**, 617–631.

Xu K., Bastia E. and Schwarzschild M. (2005) Therapeutic potential of adenosine A_{2A} receptor antagonists in Parkinson's disease. *Pharmacol. Ther.* **105**, 267–310.

Yu L., Huang Z., Mariani J., Wang Y., Moskowitz M. and Chen J. F. (2004) Selective inactivation or reconstitution of adenosine A_{2A} receptors in bone marrow cells reveals their significant contribution to the development of ischemic brain injury. *Nat. Med.* **10**, 1081–1087.

Yu L., Shen H. Y., Coelho J. E. *et al.* (2008) Adenosine A_{2A} receptor antagonists exert motor and neuroprotective effects by distinct cellular mechanisms. *Ann. Neurol.* **63**, 338–346.